Solving the Fokker-Planck kinetic equation on a lattice

Daniele Moroni,[1] Benjamin Rotenberg,[2] Jean-Pierre Hansen,[1] Sauro Succi,[3] and Simone Melchionna[4]
[1]*Department of Chemistry, University of Cambridge, Lensfield Road, Cambridge CB2 1EW, United Kingdom*
[2]*Université P. et M Curie-Paris6, UMR CNRS 7612, Laboratoire Liquides Ioniques et Interfaces Chargées, 4 place Jussieu, Paris F-75005 France*
[3]*Istituto per le Applicazioni del Calcolo "M. Picone," CNR, Viale del Policlinico 137, 00161, Rome, Italy*
[4]*INFM-SOFT, Department of Physics, University of Rome "La Sapienza," P.le A. Moro 2, 00185 Rome, Italy*
(Received 19 December 2005; published 22 June 2006)

We propose a discrete lattice version of the Fokker-Planck kinetic equation in close analogy with the lattice-Boltzmann scheme. Our work extends an earlier one-dimensional formulation to arbitrary spatial dimension D. A generalized Hermite-Gauss procedure is used to construct a discretized kinetic equation and a Chapman-Enskog expansion is applied to adapt the scheme so as to correctly reproduce the macroscopic continuum equations. The linear stability of the algorithm with respect to the finite time step Δt is characterized by the eigenvalues of the collision matrix. A heuristic second-order algorithm in Δt is applied to investigate the time evolution of the distribution function of simple model systems, and compared to known analytical solutions. Preliminary investigations of sedimenting Brownian particles subjected to an orthogonal centrifugal force illustrate the numerical efficiency of the Lattice-Fokker-Planck algorithm to simulate nontrivial situations. Interactions between Brownian particles may be accounted for by adding a standard Bhatnagar-Gross-Krook collision operator to the discretized Fokker-Planck kernel.

DOI: 10.1103/PhysRevE.73.066707 PACS number(s): 47.11.−j, 47.10.−g, 05.20.Dd

I. INTRODUCTION

Kinetic equations are well-established mathematical models for investigating the behavior out of equilibrium of fluids, and their relaxation toward thermodynamic equilibrium, at a molecular or coarse-grained, mesoscopic level [1]. They govern the time evolution of the single-particle distribution function $f(\mathbf{x},\mathbf{v};t)$ in the $(2\times D)$-dimensional space of position $\mathbf{x}$ and velocity $\mathbf{v}$. This evolution is expressed in terms of "free flow," under the action of an external or self-consistent force field, and of the action of a "collision" operator $\hat{C}[f]$, which accounts for the interactions between particles, or their coupling to a continuous medium. The exact form of the operator $\hat{C}$ involves a hierarchy of equations for the higher-order distribution functions (the Bugoliubov-Born-Green-Kirkwood-Yvon BBGKY hierarchy [2]), so that a closed equation for f cannot be obtained. Depending on the physical problem at hand, approximate closures have been devised which lead to various standard kinetic equations.

Thus, if particle interactions are only considered at a mean-field level, through a self-consistent force field, $\hat{C}\equiv 0$ and the standard Vlasov equation of plasma physics results [3]. In dilute gases of molecules interacting through short-range forces, one may make the assumption of strictly binary, uncorrelated collisions, which leads to the nonlinear Boltzmann collision operator involving the molecular scattering cross section [1]. The Boltzmann equation has been widely used for a systematic investigation of transport phenomena in gases [4], while its generalization by Enskog, which accounts for static correlations, allows such calculations to be extended to dense fluids [1].

Following the idea that the molecular details included in the Boltzmann and Enskog collision operators are not likely to have a strong influence on the experimentally measured macroscopic properties of fluids, Bhatnagar, Gross, and Krook (BGK) proposed a highly simplified, phenomenological version of the collision operator describing the relaxation of the distribution function toward local Maxwellian equilibrium on a single time scale τ. The BGK operator [5] still conserves mass, momentum, and kinetic energy, and by properly adjusting the relaxation time τ, it goes beyond the strictly binary collision assumption of the Boltzmann equation and hence allows its phenomenological extension to dense fluids [6]. The combination of the BGK kernel with discretized lattice versions of kinetic equations, globally referred to as the *lattice-Boltzmann* (LB) method [6–8] has proved to be a powerful tool for the study of laminar or turbulent fluid flow and transport. The assumption that fluid particles can be restricted to have only a small, fixed number of velocities $\mathbf{v}$ reduces the computational problem considerably compared to corresponding finite difference schemes. The numerical parameters of the lattice-BGK model can be adjusted to reproduce the correct Navier-Stokes behavior in the double limit of small Knudsen and Mach numbers (quasi-incompressible flows). Over the last decade the LB method has increased in popularity as successful applications have been repeatedly reported in numerical simulations of large-scale hydrodynamic flows [9], complex fluids under shear and in porous media [10], self-assembly into mesophases [11], ion transport in bulk solutions [12] and in nanochannels [13], liquid crystal rheology [14], and colloidal suspensions [15,16].

The latter systems generally involve a considerable separation in size and time scales as epitomized by the classic concept of Brownian motion. This is generally the case of two-component systems involving a molecular-scale solvent and larger, heavier solutes. The natural kinetic theory framework to handle such highly asymmetric situations is the Fokker-Planck (or Kramers) equation [17], which adopts an effective, one-component description of the solute, whereby the solvent and the boundaries are modeled implicitly, as

sources of friction and random forces. The collision operator $\hat{C}[f]$ may then be constructed as the sum of a Fokker-Planck (FP) operator, which accounts for the coupling between the solute and the (continuous) solvent and between the solute and the confining surfaces, and of a BGK operator to model solute-solute interactions. The corresponding lattice Fokker-Planck (LFP) equation was recently put forward by some of us [18], and applied to a simple one-dimensional problem of electrical conduction [19]. The same strategy may also apply to dilute solutions of microscopic solutes, like ions, in a solvent and provide a numerically efficient alternative to Brownian dynamics [20], or to a multicomponent LB scheme involving coupled equations for the solute and solvent distribution functions [21–23].

The main objective of the present paper is to extend the LFP formulation to the D-dimensional case, and to develop an efficient and stable numerical scheme for its solution. This should provide an operational tool to tackle nonequilibrium problems in the field of dispersions and complex fluids involving multiple length and time scales.

The paper is organized as follows. The lattice discretization of the FP equation is carried out in Sec. II. Using a truncated expansion of the distribution function $f(\mathbf{x},\mathbf{v};t)$ in generalized Hermite polynomials, the collision operator $\hat{C}[f]$ is expressed in terms of the moments of f, which can be computed by appropriate quadratures. This completely defines the LFP numerical solution scheme. In Sec. III we address the stability of such a scheme. Since the evolution of the discretized distribution functions can be rewritten as a linear iteration, studying the stability amounts to analyzing the spectrum of the transformation. A standard Chapman-Enskog expansion of the LFP equation is carried out in Sec. IV to ascertain the reproducibility of the continuous macroscopic equations. The practical implementation of a second-order algorithm in the discrete time step Δt is proposed in Sec. V, while numerical results are presented in Sec. VI. Concluding remarks are contained in Sec. VII, and mathematical issues are detailed in the appendices.

II. THE LATTICE FOKKER-PLANCK EQUATION

Since the implementation of the BGK collision operator in the LB method is well documented in the literature [6,8], we restrict the following to the Fokker-Planck operator. The standard FP kinetic equation in D dimensions reads [17]

$$(\partial_t + v_\alpha \partial_\alpha + a^E_\alpha \partial_{v_\alpha}) f = \hat{C}^{FP}[f] \doteq \gamma \partial_{v_\alpha}(v_\alpha + v_T^2 \partial_{v_\alpha}) f \quad (1)$$

where x_α and v_α are the Cartesian components of the D-dimensional position and velocity vectors $\mathbf{x}$ and $\mathbf{v}$, ∂_α and ∂_{v_α} are the corresponding gradient operators, and a^E_α are the components of the acceleration due to an external force field $m\mathbf{a}^E$ acting on the solute particles of mass m. Here and in the following greek indices run from 1 to D and we adopt Einstein's summation convention over repeated indices. The left-hand side is a conventional streaming operator, while the right-hand side is a Fokker-Planck operator with constant friction coefficient γ and thermal velocity $v_T^2 = k_B T/m$, where k_B is the Boltzmann constant and T the temperature of the system.

Equation (1) governs the approximate time evolution of the distribution function $f(\mathbf{x},\mathbf{v};t)$ of a microscopic or mesoscopic solute. The friction coefficient γ, which sets a natural inverse time scale, accounts for the coupling between the solute and the majority solvent particles, and for the friction force exerted by any confining surfaces. The force $m\mathbf{a}^E(\mathbf{x},t)$ acting on a solute particle at $\mathbf{x}$, at time t may be an external driving force, like a dc or ac electric field, or a self-consistent force due to the combined action of all other solute particles like the self-consistent electric field appearing in the Vlasov kinetic equation for plasmas, or a drag force due to solute flow. In the latter self-consistent case, the force depends on the local value of the distribution function f, so that the FP equation (1) is intrinsically nonlinear. In the present paper we focus on the simpler linear situation of an external force field to investigate solute diffusion and drift, but much of the formal development of subsequent sections remains valid in the nonlinear case.

In the lattice-Boltzmann method the continuous velocity $\mathbf{v}$ is replaced by a finite set of discrete velocities $\mathbf{v}_i$, $i = 1, \ldots, b$, which are vectors on a lattice. Accordingly, the distribution function $f(\mathbf{x},\mathbf{v};t)$ is replaced by b functions $g_i(\mathbf{x};t) \propto f(\mathbf{x},\mathbf{v}_i;t)$, and Eq. (1) by b equations for each of the g_i. In these equations the $\mathbf{v}_i$ are no longer variables, but fixed parameters. The positions $\mathbf{x}$ are discrete points on the lattice, whose size and boundaries are modeled on the geometry of the physical problem. Completing the discretization, time t is considered to evolve in multiples of a discrete step Δt. In order to derive the discrete equations, we define the external force operator

$$\hat{C}^{ext}[f] = -a^E_\alpha \partial_{v_\alpha} f \quad (2)$$

and rewrite Eq. (1) as

$$(\partial_t + v_\alpha \partial_\alpha) f = \hat{C}[f] \quad (3)$$

with $\hat{C}[f] = \hat{C}^{FP}[f] + \hat{C}^{ext}[f]$. On the left-hand side we now have a free-particle streaming operator, which can be easily discretized, as we will show in the next section. The nontrivial task is to find the correct lattice collision operator $\hat{L}$ corresponding to the continuous operator $\hat{C}$. In the BGK case, a systematic procedure has been devised in [24–26] based on Gauss-Hermite quadratures. The procedure is inspired by the pioneering ideas by Grad [27] to solve the Boltzmann equation using the so-called 13-moment system, and has become a useful tool in discrete models of the Boltzmann equation [28,29]. It relies on the fact that products of a Gaussian with Hermite polynomials are eigenfunctions of the BGK operator. We prove in the following that the Gauss-Hermite strategy also allows one to discretize the Fokker-Planck kinetic equation because BGK and FP operators share the same set of eigenfunctions. Indeed they are just different limits of a more general integral operator, devised by Skinner and Wolynes [30]. The additional force term present in $\hat{C}[f]$ is not diagonal in this basis set, but it has nevertheless a computationally convenient form. Although

the methodology is not new, its application in the FP context is the purpose of the present work. In order to provide a comprehensive and self-contained treatment we give full mathematical details in the following.

The discretization is best carried out by expanding the continuous distribution function $f(\mathbf{x},\mathbf{v};t)$ over a basis set of D-dimensional Hermite polynomial tensors $\mathcal{H}^{(l)}_{\underline{\alpha}}(\mathbf{v})$ (see Appendix A), according to

$$f(\mathbf{x},\mathbf{v};t) = \omega(\mathbf{v})\sum_{l=0}^{\infty} \frac{1}{v_T^{2l} l!} F^{(l)}_{\underline{\alpha}}(\mathbf{x},t)\mathcal{H}^{(l)}_{\underline{\alpha}}(\mathbf{v}) \tag{4}$$

where the subscript $\underline{\alpha}$ is an abbreviation for $\alpha_1,\ldots,\alpha_l$, the product denotes contraction on all l indices, and

$$\omega(\mathbf{v}) = \frac{e^{-v^2/(2v_T^2)}}{(2\pi v_T^2)^{D/2}} \tag{5}$$

is a Gaussian weight function, with $v^2=\mathbf{v}\cdot\mathbf{v}$. The expansion coefficients are given by

$$F^{(l)}_{\underline{\alpha}}(\mathbf{x},t) = \int d\mathbf{v}\, f(\mathbf{x},\mathbf{v};t)\mathcal{H}^{(l)}_{\underline{\alpha}}(\mathbf{v}) \tag{6}$$

where the velocity integrals are always taken over $\mathbb{R}^D$. Since $\mathcal{H}^{(l)}_{\underline{\alpha}}(\mathbf{v})$ involve polynomials of order l, the $F^{(l)}_{\underline{\alpha}}$ are linear combinations of the moments of f,

$$M^{(m)}_{\underline{\alpha}}(\mathbf{x},t) = \int d\mathbf{v}\, f(\mathbf{x},\mathbf{v};t) v_{\alpha_1}\cdots v_{\alpha_m}, \tag{7}$$

with $m \leqslant l$.

Inserting the expansion (4) in the kinetic equation (3), we could project the equation on the basis set and derive a hierarchy of differential equations for the coefficients. However, that would simply transform the problem into another of equivalent complexity. Here we aim instead at a different approach. By means of the Hermite expansion we can express the right-hand side of (3) as a function of the moments of f. Using a lattice-discretized distribution function we can compute these moments by a suitable quadrature. The expansion involves an infinite number of moments and clearly we have to truncate it at a certain order K. We hence *assume* that

$$F^{(l)}_{\underline{\alpha}}(\mathbf{x},t) = 0 \quad \text{if } l > K \tag{8}$$

and rewrite f as a distribution function that lies entirely in the subspace of Hermite polynomials up to order K

$$f(\mathbf{x},\mathbf{v};t) = \omega(\mathbf{v})\sum_{l=0}^{K} \frac{1}{v_T^{2l} l!} F^{(l)}_{\underline{\alpha}}(\mathbf{x},t)\mathcal{H}^{(l)}_{\underline{\alpha}}(\mathbf{v}). \tag{9}$$

This assumption is expected to be valid at least for situations close to equilibrium. Using the properties of $\hat{C}^{FP}[f]$ and $\hat{C}^{ext}[f]$ detailed in Appendix B, we also find that the outcome of $\hat{C}[f]=\hat{C}^{FP}[f]+\hat{C}^{ext}[f]$ lies entirely in this subspace.

The key idea of the lattice-Boltzmann method is that in order to compute the velocity integrals in Eq. (7), only a finite set of velocities is needed. Specifically, we want to compute D-dimensional integrals as discretized sums over a fixed set of points. We assume there exists a set of vectors $\mathbf{v}_i \in \mathbb{R}^D$, and a set of real numbers w_i, with $i=1,\ldots,b$, such that if $p(\mathbf{v})$ is a polynomial of degree not greater than $2K$, the following formula is valid:

$$\int d\mathbf{v}\, \omega(\mathbf{v})p(\mathbf{v}) = \sum_{i=1}^{b} w_i p(\mathbf{v}_i). \tag{10}$$

The above equation is then called a quadrature of degree $2K$, and the $\mathbf{v}_i$ and w_i, the nodes and weights of the quadrature.

Because of the truncated expansion Eq. (9), f/ω is a polynomial of order K at most. Since we requested a quadrature of degree $2K$ we can now compute the moments of f up to order K, according to

$$\begin{aligned}\int d\mathbf{v}\, f(\mathbf{x},\mathbf{v};t) v_{\alpha_1}\cdots v_{\alpha_m} &= \int d\mathbf{v}\frac{\omega(\mathbf{v})}{\omega(\mathbf{v})} f(\mathbf{x},\mathbf{v};t) v_{\alpha_1}\cdots v_{\alpha_m} \\ &= \sum_{i=1}^{b} w_i \frac{f(\mathbf{x},\mathbf{v}_i;t)}{\omega(\mathbf{v}_i)} v_{i\alpha_1}\cdots v_{i\alpha_m} \\ &\doteq \sum_{i=1}^{b} g_i v_{i\alpha_1}\cdots v_{i\alpha_m}\end{aligned} \tag{11}$$

where we defined $g_i(\mathbf{x};t)=w_i f(\mathbf{x},\mathbf{v}_i;t)/\omega(\mathbf{v}_i)$ and the formula is valid for $m \leqslant K$.

The choice of K is dictated by the application. In practice one is not interested in knowing f itself, but rather in computing its moments, which correspond to macroscopic observables. Momentum and energy equations involve moments up to second and third order, respectively. Consequently it is necessary to require $K \geqslant 2$ or $K \geqslant 3$. The lower-order moments are labeled by conventional names and the quadratures read

$$\rho \doteq M^{(0)} = \int d\mathbf{v}\, f(\mathbf{x},\mathbf{v};t) = \sum_{i=1}^{b} g_i, \tag{12a}$$

$$J_\alpha \doteq \rho u_\alpha \doteq M^{(1)}_\alpha = \int d\mathbf{v}\, f(\mathbf{x},\mathbf{v};t) v_\alpha = \sum_{i=1}^{b} g_i v_{i\alpha}, \tag{12b}$$

$$P_{\alpha\beta} \doteq M^{(2)}_{\alpha\beta} = \int d\mathbf{v}\, f(\mathbf{x},\mathbf{v};t) v_\alpha v_\beta = \sum_{i=1}^{b} g_i v_{i\alpha} v_{i\beta}, \tag{12c}$$

and if $K \geqslant 3$ we can also compute exactly

$$Q_{\alpha\beta\gamma} \doteq M^{(3)}_{\alpha\beta\gamma} = \int d\mathbf{v}\, f(\mathbf{x},\mathbf{v};t) v_\alpha v_\beta v_\gamma = \sum_{i=1}^{b} g_i v_{i\alpha} v_{i\beta} v_{i\gamma}. \tag{12d}$$

Finding the optimal set $\{\mathbf{v}_i, w_i\}$ in terms of a minimum number of nodes for a given degree of accuracy is in general an unsolved problem [31]. However, as far as the solutions of kinetic equations are concerned, it is also important that the $\mathbf{v}_i$ be vectors of a regular lattice in $\mathbf{x}$ space. Then for the cases of physical interest ($D=1,2,3$ and $K=2,3$) a number of possibilities exist with different b's. The thermal velocity v_T can also become a free parameter to adjust the quadra-

tures. Some resulting models that are used in practice can be found for example in [6].

We now have the prerequisites to develop a computational scheme for the Fokker-Planck kinetic equation. Consider the distribution function f evaluated at discrete lattice points $\mathbf{x}$ and at a finite set of b velocities $\mathbf{v}_i$ that are also lattice vectors. Multiplying both sides of Eq. (3) by $w_i/\omega(\mathbf{v}_i)$ and using the expansion (9) not on f but on the function $\hat{C}[f]$, we can write

$$\partial_t g_i + v_{i\alpha}\partial_\alpha g_i = w_i \sum_{l=0}^{K} \frac{1}{v_T^{2l} l!} C_{\underline{\alpha}}^{(l)} \mathcal{H}_{\underline{\alpha}}^{(l)}(\mathbf{v}_i) \tag{13}$$

where now

$$C_{\underline{\alpha}}^{(l)} = \int d\mathbf{v}\, \hat{C}[f] \mathcal{H}_{\underline{\alpha}}^{(l)}(\mathbf{v}). \tag{14}$$

The idea of using the postcollision function $\hat{C}[f]$ instead of f was introduced already in [32] to solve the Boltzmann equation with a ten-moment system leading to alternative Grad equations. Finite difference time discretization to first order [26] then leads to

$$g_i(\mathbf{x} + \mathbf{v}_i\Delta t; t + \Delta t) - g_i(\mathbf{x}; t) = \Delta t w_i \sum_{l=0}^{K} \frac{1}{v_T^{2l} l!} C_{\underline{\alpha}}^{(l)} \mathcal{H}_{\underline{\alpha}}^{(l)}(\mathbf{v}_i) \tag{15}$$

which defines the lattice Fokker-Planck equation.

The above expression must be supplemented with an operational expression for the Hermite coefficients $C_{\underline{\alpha}}^{(l)}$ of $\hat{C}[f]$. Using the results of Appendix B, they can be expressed as functions of the Hermite coefficient $F_{\underline{\alpha}}^{(l)}$ of f. We can then write $C_{\underline{\alpha}}^{(l)} = C_{\underline{\alpha}}^{(l),FP} + C_{\underline{\alpha}}^{(l),ext}$, where

$$C_{\underline{\alpha}}^{(l),FP} = -\gamma l F_{\underline{\alpha}}^{(l)}, \tag{16a}$$

$$C_{\underline{\alpha}}^{(l),ext} = a_{\alpha_1}^E F_{\alpha_2,\ldots,\alpha_l}^{(l-1)} + \cdots + a_{\alpha_l}^E F_{\alpha_1,\ldots,\alpha_{l-1}}^{(l-1)} \tag{16b}$$

and $C_{\underline{\alpha}}^{(0),ext} = 0$. The $F_{\underline{\alpha}}^{(l)}$ are related in turn to the moments $M_{\underline{\alpha}}^{(l)}$ of f by the definition of the Hermite polynomials. For $K \leqslant 3$ they read

$$F^{(0)} = \rho, \tag{17a}$$

$$F_\alpha^{(1)} = J_\alpha, \tag{17b}$$

$$F_{\alpha\beta}^{(2)} = P_{\alpha\beta} - v_T^2 \rho \delta_{\alpha\beta}, \tag{17c}$$

$$F_{\alpha\beta\gamma}^{(3)} = Q_{\alpha\beta\gamma} - v_T^2[\delta_{\alpha\beta} J_\gamma + \delta_{\alpha\gamma} J_\beta + \delta_{\beta\gamma} J_\alpha], \tag{17d}$$

where ρ, J_α, etc. are related to the g_i via the quadratures Eqs. (12).

Putting together Eqs. (15)–(17) and (12), we have then a complete numerical scheme to solve the continuous equation (3). More precisely, we have different schemes according to the choice of the order K in the Hermite expansion, which allow corresponding exact computation of the moments of f up to the same order. As an example we can write explicitly to second order ($K=2$)

$$g_i(\mathbf{x} + \mathbf{v}_i\Delta t; t + \Delta t) - g_i(\mathbf{x}; t) = \Delta t \hat{L}[g_i] \tag{18a}$$

where the lattice collision operator $\hat{L}$ reads

$$\hat{L}[g_i] = w_i \left\{ [-\gamma J_\alpha + a_\alpha^E \rho] \frac{v_{i\alpha}}{v_T^2} + [-2\gamma(P_{\alpha\beta} - v_T^2 \rho \delta_{\alpha\beta}) + a_\alpha^E J_\beta + a_\beta^E J_\alpha] \frac{v_{i\alpha} v_{i\beta} - v_T^2 \delta_{\alpha\beta}}{2 v_T^4} \right\}. \tag{18b}$$

Clearly, given the functions $g_i(\mathbf{x};t)$ at time t, one can compute the moments $\rho, J_\alpha, P_{\alpha\beta}$, and hence $\hat{L}[g_i]$. The $g_i(\mathbf{x}; t+\Delta t)$ at time $t+\Delta t$ are then obtained using the left-hand side of Eq. (18a). Note that in this way we are not calculating the distribution function f but rather $g_i = w_i f(\mathbf{x}, \mathbf{v}_i; t)/\omega(\mathbf{v}_i)$. However, the quantities of interest to be sampled are the moments of f, corresponding to hydrodynamic observables. By construction the quadratures provide them straightforwardly via Eqs. (12).

The scheme derived here defines an algorithm for the numerical solution of Eq. (3). In the case $D=1$, greek subscripts are no longer necessary, expressions (16) reduce to $C^{(l)} = -\gamma l F^{(l)} + a^E l F^{(l-1)}$, and Eqs. (17) simplify as well. These expressions coincide with those used in [18] for a second-order ($K=2$) scheme. In [18] the discrete lattice equations are tested against the continuous equation only numerically. In this paper we improve the analysis of the scheme and address also analytically its stability and the reproducibility of the continuous equation (3). A discussion of the computational algorithm is then given in Sec. V.

III. STABILITY ANALYSIS

In the following we show that Eq. (15) can be recast in the linear form

$$g_i' = \sum_j \bar{C}_{ij} g_j \tag{19}$$

where $g_i' = g_i(\mathbf{x} + \mathbf{v}_i\Delta t; t+\Delta t) - g_i(\mathbf{x}; t)$ defines a vector g', $g_j = g_j(\mathbf{x}, t)$ a vector g, and $\bar{C}_{ij}$ the so-called collision matrix $\bar{C}$ [6,33,34]. For a given lattice geometry, $\bar{C}$ is a constant matrix that depends only on the operator parameters γ, a_α^E. In particular we consider isothermal models, where v_T is fixed and we make the relatively strong assumption that the external acceleration field $\mathbf{a}^E$ does not depend self-consistently on the distribution functions g_i. The latter case will be examined in a subsequent publication.

The aim of this section is to check for which range of these parameters the scheme embodied in Eq. (19) is stable, where stability means that upon iterating the scheme, the distribution functions $g_i(\mathbf{x};t)$ stay finite at any value of $\mathbf{x}$ and t. The task is significantly eased by the fact that we do not have to first linearize the scheme, as in the usual Von Neumann stability analysis [8]. By standard arguments in lattice-Boltzmann theory [7] the stability condition reads

$$|1+\lambda(\bar{C})|<1 \tag{20}$$

where $\lambda(\bar{C})$ is any eigenvalue of $\bar{C}$. We remark that Eq. (20) is a very simple condition valid globally, independently of the initial distributions $g_i(\mathbf{x};0)$ or the boundary geometry. Such a feature is an attractive consequence of the linearity of the scheme, while much more complicated stability analyses which depend on the local $g_i(\mathbf{x};0)$ are required in the full self-consistent LB method [35].

Thanks to Eq. (20) the stability analysis reduces to the spectral analysis of $\bar{C}$. We proceed now to first identify this matrix, and then compute its spectrum using the results of the previous section.

As a starting point, we rewrite Eq. (15) as

$$g_i'/\Delta t = w_i \sum_{l=1}^{n} \frac{1}{N_l^2} C^{(l)} \mathcal{H}^{(l)}(\mathbf{v}_i) \tag{21}$$

where temporarily in this section we set aside the tensorial notation and enumerate all the terms of the sum (including the tensorial contraction) simply from 1 to n. As a result, the index l here represents a shorthand notation for the previous set of indices $l\underline{\alpha}$. Accordingly we redefine the normalization factors as just N_l^2, since it is not necessary to know their detailed form. We wish then to express Eq. (21) in the matrix form of Eq. (19) using the fact that the dependence on $g_i=w_i f_i/\omega(\mathbf{v}_i)$ is inside $C^{(l)}=\int d\mathbf{v}\, \hat{C}[f]\mathcal{H}^{(l)}(\mathbf{v})$.

The first step is then to use the quadratures to write (see Appendix A)

$$\sum_i w_i \mathcal{H}^{(l)}(\mathbf{v}_i)\mathcal{H}^{(m)}(\mathbf{v}_i) = \delta_{lm} N_l^2. \tag{22}$$

Defining the matrix $H_{il} \doteq \mathcal{H}^{(l)}(\mathbf{v}_i)$ (which contains b rows times n columns), Eq. (22) is rewritten in matrix form

$$H^T W H = N^2 \tag{23}$$

where H^T is the transpose of H, $W_{ij} \doteq w_i \delta_{ij}$ is a $b\times b$ diagonal matrix, and $N^2=N_l^2\delta_{lm}$ is an $n\times n$ diagonal matrix. Stated otherwise $H^T(WHN^{-2})=I$, i.e., WHN^{-2} is a right-inverse $(H^T)^{-1,R}$ of H^T.

As a second step, we consider the operator $\hat{C}$, and we apply it to f expanded in its Hermite representation,

$$\hat{C}\circ f = \hat{C}\circ\left(\omega(\mathbf{v})\sum_{l=1}^{n}\frac{1}{N_l^2}F^{(l)}\mathcal{H}^{(l)}(\mathbf{v})\right) = \sum_{l=1}^{n}\hat{C}\circ\left(\omega(\mathbf{v})\frac{\mathcal{H}^{(l)}(\mathbf{v})}{N_l^2}\right)F^{(l)} \tag{24}$$

where $F^{(l)}=\int d\mathbf{v}\, f\mathcal{H}^{(l)}(\mathbf{v})$. Upon projecting along $\mathcal{H}^{(m)}(\mathbf{v})$ we get

$$C^{(m)} = \int d\mathbf{v}\, \mathcal{H}^{(m)}(\mathbf{v})[\hat{C}\circ f] = \sum_{l=1}^{n}\left[\int d\mathbf{v}\, \mathcal{H}^{(m)}(\mathbf{v})\hat{C}\circ\left(\omega(\mathbf{v})\frac{\mathcal{H}^{(l)}(\mathbf{v})}{N_l^2}\right)\right]F^{(l)} = \sum_{l=1}^{n} C_{ml}F^{(l)}, \tag{25}$$

where the quantity in large square brackets defines the elements C_{ml} of an $n\times n$ matrix C.

The third step is to express $F^{(l)}$ in terms of the g_i:

$$F^{(l)} = \int d\mathbf{v}\, f\mathcal{H}^{(l)}(\mathbf{v}) = \int d\mathbf{v}\, \omega(\mathbf{v})\frac{f}{\omega(\mathbf{v})}\mathcal{H}^{(l)}(\mathbf{v}) = \sum_i w_i \frac{f_i}{\omega(\mathbf{v}_i)}\mathcal{H}^{(l)}(\mathbf{v}_i) = \sum_i g_i \mathcal{H}^{(l)}(\mathbf{v}_i), \tag{26}$$

where the last term can be rewritten in matrix notation as $H^T g$.

Combining the results obtained in the above three steps we can write (21) in matrix form

$$g'/\Delta t = WHN^{-2}CH^T g \tag{27}$$

which identifies the collision matrix

$$\bar{C}/\Delta t = WHN^{-2}CH^T = (H^T)^{-1,R}CH^T. \tag{28}$$

For clarity we can equivalently write $H^T_{nb}\bar{C}_{bb}=\Delta t C_{nn}H^T_{nb}$ where the matrix dimensions are indicated by explicit subscripts.

Equation (28) is a representation of the collision matrix that allows its spectral analysis. Indeed the spectrum of $\bar{C}$ is directly connected to that of C. In the square case $n=b$ the two matrices are similar and have the same spectrum. In the general rectangular case, since $b\geqslant n$, the spectrum of C is contained in the spectrum of $\bar{C}$ [an eigenvector of $\bar{C}$ being just $(H^T)^{-1,R}v$ where v is an eigenvector of C]. The additional $b-n$ eigenvalues are just 0.

We have therefore reduced the problem to the computation of the spectrum of C. We can deduce an explicit representation of this matrix using relations (16) and the defining equation (25). The matrix C reads

$$\begin{pmatrix} 0 & & & \\ & -\gamma & & \\ (\mathbf{a}^E) & \ddots & & \\ & & -\gamma & \\ & (\mathbf{a}^E) & & -2\gamma \\ & & & \ddots \\ & & & & -2\gamma \\ & & & & & \ddots \end{pmatrix} \tag{29}$$

where $(\mathbf{a}^E)$ contains only a_α^E components, the square matrices are diagonal, and all the remaining elements are zero. The Fokker-Planck operator fills the diagonal while $\hat{C}^{ext}$ occupies the lower diagonal part. The resulting matrix is triangular and the eigenvalues are just given by the diagonal elements, independently of the off-diagonal ones, i.e.,

$$\lambda_k = -\gamma k, \quad k = 0, \ldots, K. \tag{30}$$

Consequently, the collision matrix $\bar{C}$ has eigenvalues $\lambda_k \Delta t$. Going back to conditions (20), the most stringent one is for $k=K$ and reads

$$0 < \gamma \Delta t < 2/K \tag{31}$$

which in the case of the $K=2$ scheme of Eq. (18) reduces to $0 < \gamma \Delta t < 1$. These inequalities completely identify the range of model parameters for which the scheme proposed in Sec. II does not lead to an unbounded growth of the distribution functions with time. Note that the stability requirement imposes conditions only on the parameter γ independently of the external field $\mathbf{a}^E$. This is due to the initial assumption that the field does not depend on the g_i. We expect this conclusion not to be valid numerically, as very strong fields would lead to high-Mach-number regimes where lattice-Boltzmann schemes are known to break down [6] (with the possible exception of entropic schemes [28,29]). To this purpose we validate the range of applicability derived in this section with numerical simulations in Sec. VI. Inclusion of self-consistent force fields, that depend for example on the local density Eq. (12a), would require a more careful analysis [35].

IV. CHAPMAN-ENSKOG EXPANSION

A kinetic equation describes a system at the microscopic level of the distribution function $f(\mathbf{x}, \mathbf{v}; t)$. Define the Knudsen number ϵ as the ratio of the mean distance between two successive particle collisions and the characteristic spatial scale of the system (e.g., radius of an obstacle in a flow). If this number is very small the details of particle collisions can be neglected and the system can be regarded as a continuum. Using the Knudsen number as an expansion parameter, Chapman and Enskog were able to derive from the Boltzmann equation the evolution of the hydrodynamic variables (corresponding to the lower order moments of f) in the continuum limit, thus reproducing the macroscopic Navier-Stokes equations [1]. Eventually, the expansion has also been used in the context of the LB method to derive the macroscopic equations obeyed by lattice-Boltzmann models. The fundamental hydrodynamic equations were recovered consistently [36].

The Chapman-Enskog procedure is not restricted to the Boltzmann and lattice-Boltzmann equations. In this section we apply it to the continuous Fokker-Planck kinetic equation (3) and to the second-order ($K=2$) lattice scheme of Eq. (18). We can then check if the same macroscopic equations for the first moments are reproduced.

In the continuous case the expansion is straightforward. Indeed one can avoid it completely and obtain the equations for the macroscopic variables by just multiplying Eq. (3) by $v_{\alpha_1} \cdots v_{\alpha_m}$ and integrating over velocity space. In general at order m, one obtains the time derivative of the mth moment plus the divergence of its flux on the left-hand side. On the right-hand side the moments of $\hat{C}[f]$ can be calculated using the Hermite expansion and the properties of Hermite polynomials, as was done in the previous section to compute the collision matrix. Explicitly, up to order 1, the result is

$$\partial_t \rho + \partial_\alpha J_\alpha = 0, \tag{32a}$$

$$\partial_t J_\alpha + \partial_\beta P_{\alpha\beta} = -\gamma (J_\alpha - \rho u_\alpha^E) \tag{32b}$$

where we have introduced the *external velocity* $u_\alpha^E = a_\alpha^E / \gamma$. The first is the continuity equation; the second gives the evolution of the first moment J_α, but involves also the unknown second moment $P_{\alpha\beta}$. Indeed this procedure simply generates a nonclosed hierarchy of equations for the moments of f. However, we are not interested here in reproducing the Navier-Stokes equations, nor are we interested in obtaining a closed set of equations. What we wish to check in the following is whether the lattice scheme of Sec. II actually reproduces the same hierarchy of equations of the continuous case.

In the discrete case we must make use of the complete Chapman-Enskog expansion. To make it more transparent we have divided this derivation into subsections.

A. Preliminaries

The macroscopic phenomena that we aim at reproducing can occur on different time and spatial scales. For example, there may be elastic effects, such as sound propagation, on short time scales, and viscous effects, such as damping, on longer time scales. The idea of the Chapman-Enskog expansion is that assuming such a separation of scales, these phenomena can be analyzed with multiscale asymptotic methods [37]. We hence expand the populations g_i and the spatial and time derivatives in powers of the Knudsen number parameter ϵ. The hydrodynamic limit corresponds to $\epsilon \ll 1$. In this limit, noticeable spatial variations take place typically over distances of order ϵ^{-1}. It is hence natural to introduce a macroscopic space variable defined as $\mathbf{x}_1 = \epsilon \mathbf{x}$. Since we expect both propagation and diffusion phenomena, we must expand up to second order in time, because in diffusion processes inhomogeneities at the ϵ^{-1} space scale will relax on the ϵ^{-2} time scale. Therefore we introduce two time variables $t_1 = \epsilon t$ and $t_2 = \epsilon^2 t$. As usual in multiscale methods, we then write

$$g_i = g_i^{(0)} + \epsilon g_i^{(1)} + \epsilon^2 g_i^{(2)}, \tag{33}$$

$$\partial_t = \epsilon \partial_t^{(1)} + \epsilon^2 \partial_t^{(2)}, \tag{34}$$

$$\partial_\alpha = \epsilon \partial_\alpha^{(1)}. \tag{35}$$

Equation (33) defines a corresponding expansion of the moments of g as

$$\rho = \sum_i g_i = \sum_i [g_i^{(0)} + \epsilon g_i^{(1)} + \epsilon^2 g_i^{(2)}] \doteq \rho^{(0)} + \epsilon\rho^{(1)} + \epsilon^2\rho^{(2)} \tag{36}$$

and similarly for $J_\alpha, P_{\alpha\beta}$. For convenience we also rewrite the lattice collision operator Eq. (18b) as

$$\hat{L}[g_i] = -\gamma \bar{J}_\alpha \frac{v_{i\alpha}}{v_T^2} w_i - 2\gamma \bar{P}_{\alpha\beta} \frac{v_{i\alpha}v_{i\beta} - v_T^2\delta_{\alpha\beta}}{2v_T^4} w_i \tag{37}$$

where

$$\bar{J}_\alpha \doteq J_\alpha - \rho u_\alpha^E, \tag{38}$$

$$\bar{P}_{\alpha\beta} \doteq P_{\alpha\beta} - v_T^2\rho\delta_{\alpha\beta} - \frac{1}{2}(u_\alpha^E J_\beta + u_\beta^E J_\alpha). \tag{39}$$

Since $\bar{J}_\alpha$ and $\bar{P}_{\alpha\beta}$ depend linearly on the moments ρ, J_α, $P_{\alpha\beta}$, we can write for them an expansion similar to Eq. (36); namely, $\bar{J}_\alpha = \bar{J}_\alpha^{(0)} + \epsilon\bar{J}_\alpha^{(1)} + \epsilon^2\bar{J}_\alpha^{(2)}$ and analogously for $\bar{P}_{\alpha\beta}$.

B. Expansion details

The first step is to apply the expansions defined in the previous subsection to both sides of Eq. (18). On the left-hand side, we first manipulate the streaming operator as usual in Chapman-Enskog expansions for lattice-Boltzmann models [8]. Since the scale expansion parameter ϵ is small, the populations vary little from one node the next. We can approximate the population $g_i(\mathbf{x}+\mathbf{v}_i\Delta t; t+\Delta t)$ by its Taylor expansion around $g_i(\mathbf{x};t)$, and write up to second order in Δt

$$g_i(\mathbf{x}+\mathbf{v}_i\Delta t; t+\Delta t) - g_i(\mathbf{x};t) = \Delta t\left(\partial_t + v_{i\alpha}\partial_\alpha + \frac{\Delta t}{2}(\partial_t + v_{i\alpha}\partial_\alpha) \times (\partial_t + v_{i\beta}\partial_\beta)\right) g_i(\mathbf{x};t). \tag{40}$$

Using next Eqs. (40) and (33)–(35), the streaming term $[g_i(\mathbf{x}+\mathbf{v}_i\Delta t; t+\Delta t) - g_i(\mathbf{x};t)]/\Delta t$ can be expanded in powers of ϵ as

$$\text{order } \epsilon^0, \quad 0, \tag{41}$$

$$\text{order } \epsilon^1, \quad [\partial_t^{(1)} + v_{i\alpha}\partial_\alpha^{(1)}] g_i^{(0)}, \tag{42}$$

$$\text{order } \epsilon^2, \quad [\partial_t^{(1)} + v_{i\alpha}\partial_\alpha^{(1)}] g_i^{(1)} + \left(\partial_t^{(2)} + \frac{\Delta t}{2}(\partial_t^{(1)} + v_{i\alpha}\partial_\alpha^{(1)}) \times (\partial_t^{(1)} + v_{i\beta}\partial_\beta^{(1)})\right) g_i^{(0)}. \tag{43}$$

On the right-hand side, in the case of the lattice collision operator, the expansion acts order by order on the moments and we can write

$$\hat{L}[g_i] = \hat{L}_i^{(0)} + \epsilon\hat{L}_i^{(1)} + \epsilon^2\hat{L}_i^{(2)} \tag{44}$$

where

$$\hat{L}_i^{(k)} = -\gamma \bar{J}_\alpha^{(k)} \frac{v_{i\alpha}}{v_T^2} w_i - 2\gamma \bar{P}_{\alpha\beta}^{(k)} \frac{v_{i\alpha}v_{i\beta} - v_T^2\delta_{\alpha\beta}}{2v_T^4} w_i \tag{45}$$

for $k=0$, 1, and 2.

The second step is to equate corresponding orders of the expansion. Thus we obtain to order ϵ^0

$$0 = -\gamma \bar{J}_\alpha^{(0)} \frac{v_{i\alpha}}{v_T^2} w_i - 2\gamma \bar{P}_{\alpha\beta}^{(0)} \frac{v_{i\alpha}v_{i\beta} - v_T^2\delta_{\alpha\beta}}{2v_T^4} w_i, \tag{46}$$

to order ϵ^1

$$\partial_t^{(1)} g_i^{(0)} + v_{i\alpha}\partial_\alpha^{(1)} g_i^{(0)} = -\gamma \bar{J}_\alpha^{(1)} \frac{v_{i\alpha}}{v_T^2} w_i - 2\gamma \bar{P}_{\alpha\beta}^{(1)} \frac{v_{i\alpha}v_{i\beta} - v_T^2\delta_{\alpha\beta}}{2v_T^4} w_i, \tag{47}$$

and to order ϵ^2 the equation can be rewritten more conveniently as

$$\partial_t^{(1)} g_i^{(1)} + \partial_\alpha^{(1)} v_{i\alpha} g_i^{(1)} + \partial_t^{(2)} g_i^{(0)} + \frac{\Delta t}{2}[\partial_t^{(1)}(\partial_t^{(1)} g_i^{(0)} + \partial_\beta^{(1)} v_{i\beta} g_i^{(0)}) + \partial_\alpha^{(1)}(\partial_t^{(1)} v_{i\alpha} g_i^{(0)} + \partial_\beta^{(1)} v_{i\alpha} v_{i\beta} g_i^{(0)})] = -\gamma \bar{J}_\alpha^{(2)} \frac{v_{i\alpha}}{v_T^2} w_i - 2\gamma \bar{P}_{\alpha\beta}^{(2)} \frac{v_{i\alpha}v_{i\beta} - v_T^2\delta_{\alpha\beta}}{2v_T^4} w_i. \tag{48}$$

The third step is to compute the moment equations associated with Eqs. (46) and (47). For the zeroth-moment equation one can just sum both sides of the equations over i, for the next moments one must first multiply by $v_{i\gamma}$, $v_{i\gamma}v_{i\delta}$, and so on. Note that the orders of the velocity moments are not the orders of the ϵ expansion. For each order in ϵ we can compute different moment equations. As we will show shortly, for the purpose of reproducing the macroscopic equations (32) we need up to the second-moment equation for orders ϵ^0 and ϵ^1 and only up to the first-moment equation for order ϵ^2. The computations are carried out using the relations of Appendix A. To order ϵ^0, the zeroth moment does not give any information; the first and second moments read

$$0 = -\gamma \bar{J}_\gamma^{(0)}, \tag{49a}$$

$$0 = -2\gamma \bar{P}_{\gamma\delta}^{(0)}. \tag{49b}$$

To order ϵ^1 we find for the zeroth, first, and second order moments:

$$\partial_t^{(1)}\rho^{(0)} + \partial_\alpha^{(1)} J_\alpha^{(0)} = 0, \tag{50a}$$

$$\partial_t^{(1)} J_\gamma^{(0)} + \partial_\alpha^{(1)} P_{\alpha\gamma}^{(0)} = -\gamma \bar{J}_\gamma^{(1)}, \tag{50b}$$

$$\partial_t^{(1)} P_{\gamma\delta}^{(0)} + \partial_\alpha^{(1)} Q_{\alpha\gamma\delta}^{(0)} = -2\gamma \bar{P}_{\gamma\delta}^{(1)}. \tag{50c}$$

And to order ϵ^2 we consider only the zeroth- and first-moment equations:

$$\partial_t^{(2)}\rho^{(0)} + \partial_t^{(1)}\rho^{(1)} + \partial_\alpha^{(1)} J_\alpha^{(1)} - \frac{\gamma\Delta t}{2}\partial_\alpha^{(1)}\bar{J}_\alpha^{(1)} = 0, \tag{51a}$$

$$\partial_t^{(2)} J_\gamma^{(0)} + \partial_t^{(1)} J_\gamma^{(1)} + \partial_\alpha^{(1)} P_{\alpha\gamma}^{(1)} + \frac{\Delta t}{2}[\partial_t^{(1)}(-\gamma \bar{J}_\gamma^{(1)}) + \partial_\alpha^{(1)}(-2\gamma \bar{P}_{\alpha\gamma}^{(1)})]$$

$$= -\gamma \bar{J}_\gamma^{(2)}, \tag{51b}$$

where we made use of Eqs. (50a) and (50b) to derive the first, and of Eqs. (50b) and (50c) for the second equation.

C. Macroscopic equations

We can now add up the equations at different orders in ϵ and obtain expanded macroscopic equations for the zeroth and first moments of the populations g_i. The final step then is to reconstruct the derivative operators from the expanded ones.

For the zeroth moment, we construct $\epsilon^1\times$ [Eq. (50a)] $+\epsilon^2\times$ [Eq. (51a)] (order ϵ^0 does not add anything in this case) and we get

$$\epsilon \partial_t^{(1)} \rho^{(0)} + \epsilon \partial_\alpha^{(1)} J_\alpha^{(0)} + \epsilon^2 \partial_t^{(2)} \rho^{(0)} + \epsilon^2 \partial_t^{(1)} \rho^{(1)} + \epsilon^2 \partial_\alpha^{(1)} J_\alpha^{(1)}$$

$$- \epsilon^2 \frac{\gamma \Delta t}{2} \partial_\alpha^{(1)} \bar{J}_\alpha^{(1)} = 0. \tag{52}$$

For the first moment, we construct $\epsilon^0\times$ [Eq. (49a)] $+\epsilon^1\times$ [Eq. (50b)] $+\epsilon^2\times$ [Eq. (51b)] and we obtain

$$\epsilon \partial_t^{(1)} J_\gamma^{(0)} + \epsilon \partial_\alpha^{(1)} P_{\alpha\gamma}^{(0)} + \epsilon^2 \partial_t^{(2)} J_\gamma^{(0)} + \epsilon^2 \partial_t^{(1)} J_\gamma^{(1)} + \epsilon^2 \partial_\alpha^{(1)} P_{\alpha\gamma}^{(1)}$$

$$+ \epsilon^2 \frac{\Delta t}{2}[\partial_t^{(1)}(-\gamma \bar{J}_\gamma^{(1)}) + \partial_\alpha^{(1)}(-2\gamma \bar{P}_{\alpha\gamma}^{(1)})]$$

$$= -\epsilon \gamma \bar{J}_\gamma^{(1)} - \epsilon^2 \gamma \bar{J}_\gamma^{(2)}. \tag{53}$$

In these equations both the moments of g_i (corresponding to the macroscopic variables) and the differential operators are expanded up to order ϵ^2. We can straightforwardly reconstruct the original quantities using relation (36) and the analogous ones for the other variables. The spatial derivative is reconstructed in the same spirit noting that $\partial_\alpha X = \epsilon \partial_\alpha^{(1)} \times (X^{(0)} + \epsilon X^{(1)}) = \epsilon \partial_\alpha^{(1)} X^{(0)} + \epsilon^2 \partial_\alpha^{(1)} X^{(1)}$, where X is any of the moments. In a similar fashion, for the time derivatives $\partial_t X = \epsilon \partial_t^{(1)} X^{(0)} + \epsilon^2 \partial_t^{(2)} X^{(0)} + \epsilon^2 \partial_t^{(1)} X^{(1)}$, where a term of order ϵ^3 was omitted. Inserting Eqs. (49a) and (49b) where necessary, Eqs. (52) and (53) can then be rewritten as

$$\partial_t \rho + \partial_\alpha J_\alpha = \frac{\gamma \Delta t}{2} \partial_\alpha (J_\alpha - \rho u_\alpha^E), \tag{54a}$$

$$\partial_t J_\alpha + \partial_\beta P_{\alpha\beta} = -\gamma (J_\alpha - \rho u_\alpha^E) + \gamma \Delta t \partial_\beta \Big(P_{\alpha\beta} - v_T^2 \rho \delta_{\alpha\beta}$$

$$- \frac{1}{2}(u_\alpha^E J_\beta + u_\beta^E J_\alpha) \Big) + \frac{\gamma \Delta t}{2} \partial_t (J_\alpha - \rho u_\alpha^E). \tag{54b}$$

Interestingly, we find that these equations differ from the continuous equations by one additional term in the first and by two terms in the second. All corrections are of order $\gamma \Delta t$.

We can gain more insight in these results by rewriting them in a slightly different way. Let g_i^{eq} be the solutions of $\hat{L}[g_i] = 0$. From the explicit form (37) we see that the g_i^{eq} satisfy $\bar{J}_\alpha = \bar{P}_{\alpha\beta} = 0$, or equivalently

$$J_\alpha = \rho u_\alpha^E \doteq J_\alpha^{eq}, \tag{55}$$

$$P_{\alpha\beta} = v_T^2 \rho \delta_{\alpha\beta} + \frac{1}{2}(u_\alpha^E J_\beta + u_\beta^E J_\alpha) \doteq P_{\alpha\beta}^{eq}. \tag{56}$$

With these definitions we can rewrite Eqs. (54) as

$$\partial_t \rho + \partial_\alpha J_\alpha = \frac{\gamma \Delta t}{2} \partial_\alpha (J_\alpha - J_\alpha^{eq}), \tag{57a}$$

$$\partial_t J_\alpha + \partial_\beta P_{\alpha\beta} = -\gamma (J_\alpha - J_\alpha^{eq}) + \gamma \Delta t \partial_\beta (P_{\alpha\beta} - P_{\alpha\beta}^{eq})$$

$$+ \frac{\gamma \Delta t}{2} \partial_t (J_\alpha - J_\alpha^{eq}). \tag{57b}$$

This form shows that for a given value of γ, the closer to equilibrium the system is, the closer the evolution of the discrete system is to that of the continuous Fokker-Planck equation.

Equations (57) are the final outcome of the Chapman-Enskog expansion of the numerical scheme of Eqs. (18). Together with the stability results of Sec. III, they complete the analysis of the proposed numerical method. Unfortunately, they prove that the scheme does not actually solve the continuous kinetic equation (3), because of the additional terms in Eqs. (57) with respect to Eqs. (32). However, as just illustrated, we know explicitly the error made. In the next section we exploit this knowledge to build a corrected scheme that is able to solve the continuous equation.

V. LATTICE FOKKER-PLANCK ALGORITHM

Having in mind the results of the previous section we provide here a corrected numerical procedure to solve the continuous Fokker-Planck kinetic equation (1).

The results of the Chapman-Enskog expansion suggest that by properly redefining the hydrodynamic variables it is possible to recover the correct continuous macroscopic equations. Let

$$J_\alpha^* = \left(1 - \frac{\gamma \Delta t}{2}\right) J_\alpha + \frac{\gamma \Delta t}{2} J_\alpha^{eq}, \tag{58a}$$

$$P_{\alpha\beta}^* = (1 - \gamma \Delta t) P_{\alpha\beta} + \gamma \Delta t P_{\alpha\beta}^{eq}. \tag{58b}$$

Then Eqs. (57) are rewritten as

$$\partial_t \rho + \partial_\alpha J_\alpha^* = 0, \tag{59a}$$

$$\partial_t J_\alpha^* + \partial_\beta P_{\alpha\beta}^* = -\tilde{\gamma}(J_\alpha^* - \rho u_\alpha^E), \tag{59b}$$

where an effective friction

$$\frac{1}{\tilde{\gamma}} = \frac{1}{\gamma} - \frac{\Delta t}{2} \tag{60}$$

is introduced. At the level of the Chapman-Enskog expansion the above equations correspond to the continuous Eqs. (32).

A similar approach was used in [15,38] by redefinition of velocity in the presence of a forcing term. The quantities J^*_α and $P^*_{\alpha\beta}$ reduce to J_α and $P_{\alpha\beta}$ in the limit $\gamma\Delta t \to 0$. Furthermore, if $J_\alpha = J^{eq}_\alpha = \rho u^E_\alpha$ we also have $J^*_\alpha = J_\alpha = J^{eq}_\alpha$ (and the same for the stress tensor). With walls these equalities do not hold in general. Indeed, the boundary conditions set $J^*_\alpha = 0$, whereas J^{eq}_α is nonzero when a field is applied.

A computational algorithm to solve (1) can be divided into two parts; the first initializes the simulation, and the second is the dynamical evolution of the g_i.

Initialization. If we perform a simulation using the "bare" definition of the moments in the collision operator, but sample the "corrected" moments ρ, J^*_α, and $P^*_{\alpha\beta}$, the latter satisfy the continuous Fokker-Planck equation with second-order accuracy [see Eq. (59)], but with a rescaled friction $\tilde{\gamma}$. Suppose we want to simulate a system with a friction γ_0. Then in Eq. (60) we identify $\tilde{\gamma}$ with γ_0, solve for γ, obtaining

$$\gamma = \frac{\gamma_0}{1 + \dfrac{\gamma_0 \Delta t}{2}}, \tag{61}$$

and use this γ in the simulation. The external velocity u^E_α must remain unaffected. So if one wants to apply a field $a^E_{0,\alpha}$, one must use in the simulation a field a^E_α such that $a^E_\alpha/\gamma = a^E_{0,\alpha}/\gamma_0$. The initial conditions are set on the starred variables, defined by (58) using γ, not γ_0.

Simulation loop. Given the set of $g_i(\mathbf{x};t)$ at time t, the $g_i(\mathbf{x};t+\Delta t)$ at time $t+\Delta t$ are found, for each $\mathbf{x}$, by the following steps: (1) compute the moments of f using (11), or explicitly (12), (2) compute the Hermite coefficients of f, Eq. (17), (3) compute the Hermite coefficients of $\hat{C}[f]$, Eq. (16), (4) compute the right-hand side of (15), and (5) compute the left-hand side of (15).

Then the procedure is repeated at each time step. At regular times we can sample the hydrodynamic observables of interest corresponding to the moments of f. One has to take care, however, to sample the starred variables, because these are the ones that correctly reproduce the continuous equations.

An extensive literature is available for the implementation of the lattice-Boltzmann method, where important issues such as boundary conditions and large-scale code optimization have been investigated in depth [6]. Most of the LB techniques can be directly extended to the lattice Fokker-Planck method. For further details the interested reader should consult more specialized articles, such as the performance studies of [39,40].

VI. NUMERICAL RESULTS

A. Numerical limits

Combining the results of Secs. III and IV, one finds that the second-order scheme of the previous section allows one to solve the FP equation for $0 < \gamma\Delta t < 1$, independently of the external field $\mathbf{a}^E$, and the smaller $\gamma\Delta t$, the closer the lattice solution will be to the continuous one. Moreover, since in the numerical scheme we use the friction γ given by Eq. (61) instead of the real γ_0, the stability condition actually corresponds to $0 < \gamma_0\Delta t < 2$, so that it seems possible to simulate systems with a time step longer than the reciprocal friction. These theoretical findings need some numerical backup. For this purpose we consider here two basic examples in $D=1$ for which analytical solutions are also available and we compare these solutions with the outcome of simulations in the D1Q3 lattice [6]. We can then check the validity of the proposed scheme and set constraints on the range of parameters.

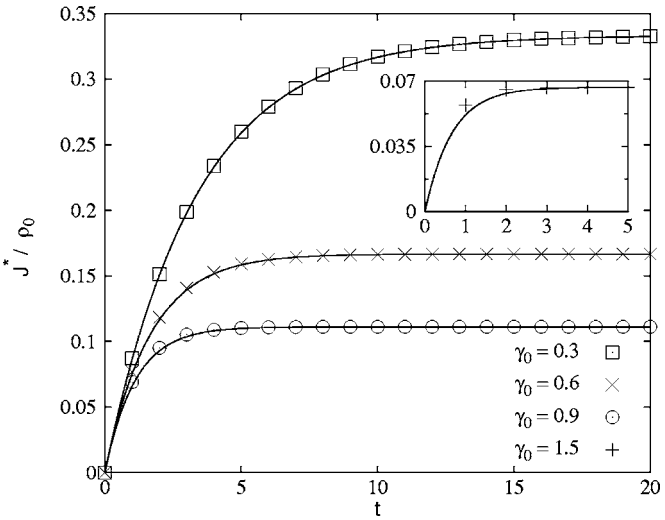

FIG. 1. Time dependence of the flux of solute particles induced by a constant external field. The system is described by the 1D FP equation (1) with acceleration $a^E_0 = 0.1\Delta x/\Delta t^2$ and periodic boundary conditions. Initially, the density is set homogeneously at ρ_0 and the velocity field to zero. The symbols display the solution of the equation using the LFP algorithm of Sec. V, while the full curves represent the analytical solution Eq. (62). In the regime $0 < \gamma_0\Delta t < 1$ the algorithm reproduces the analytical solution perfectly, while in the regime $\gamma_0\Delta t > 1$ (inset) it shows some discrepancies. Time t is in units of Δt and the vertical axis has units of $\Delta x/\Delta t$ where Δx is the lattice spacing. Friction γ_0 is in units of $1/\Delta t$.

In the first example, we consider a system with periodic boundary conditions, initially homogeneous at density ρ_0, and with zero initial velocity. A constant homogeneous field is applied resulting in an external acceleration a^E_0. From the solution of the continuous equations (32), the density does not evolve, while the flux J is uniform and evolves as

$$J = (\rho_0 a^E_0/\gamma_0)(1 - e^{-\gamma_0 t}). \tag{62}$$

Direct simulation of the system without the $\tilde{\gamma}$ prescription of Sec. V leads to an exponential solution with a wrong rate. Including the prescription and sampling the starred moment J^*, one obtains the correct result, as shown in Fig. 1. However, for $\gamma_0\Delta t \geq 1$ ($\gamma\Delta t \geq 2/3$), we find that the numerical results deviate from the continuous solution, so that, although larger time steps could be used in principle it is necessary in practice to constrain also the friction γ_0 to the range $0 < \gamma_0\Delta t < 1$.

In the second example, we consider the same system, but with bounce-back no-slip reflecting boundary conditions [6].

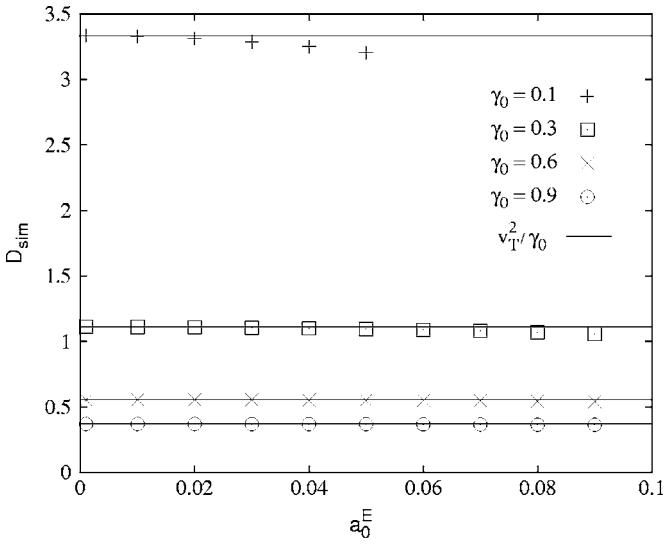

FIG. 2. Diffusion coefficient D_{sim} of solutes as a function of the constant external acceleration a_0^E. The system is described by the 1D FP equation (1) with reflecting boundaries, and is initially set to homogeneous density and vanishing velocity field. The density converges to the barometric law Eq. (63) from which the simulation estimate D_{sim} can be extracted as explained in the text. The continuous lines correspond to Einstein's relation. The deviation are caused by the discretized solution and can be explained with the results of the Chapman-Enskog expansion. The acceleration is in units $\Delta x/\Delta t^2$ and the diffusion coefficients in units $\Delta x^2/\Delta t$, where Δx is the lattice spacing, and Δt the time unit. Friction γ_0 is in units of $1/\Delta t$.

A constant field is applied resulting in an external acceleration a_0^E. Accumulation due to migration results in a concentration gradient which is the source of a diffusive flux opposed to the applied field. From the balance of fluxes, we find at equilibrium the barometric law for the density

$$\rho_{eq}(x) \propto \exp\left(\frac{a_0^E}{v_T^2}x\right) \tag{63}$$

where $v_T^2 = k_B T/m$ is the thermal velocity. The same result is obtained from the direct solution of Eqs. (32) on the assumption that the tensor $P_{\alpha\beta}$ has already relaxed to its equilibrium value $P_{\alpha\beta}^{eq}$ given by Eq. (56). Simulations without the $\tilde{\gamma}$ prescription give an exponential profile, but the exponential slope erroneously exhibits a dependence on the friction γ_0. With the correct prescription the profile is still exponential, and in order to check the slope, we first rewrite the fraction in the right-hand side of (63) as $a_0^E/(\gamma_0 D_0)$ where, from Einstein's relation, $D_0 = v_T^2/\gamma_0$. From an exponential fit of our data we can then derive a simulated diffusion coefficient D_{sim} upon dividing a_0^E/γ_0 by the measured slope. The numerical results are reported in Fig. 2 compared to the continuous value D_0. Slight deviations can be observed, especially for small γ_0. These findings can be understood from the Chapman-Enskog analysis. At steady state, Eqs. (59) become

$$\partial_\alpha J_\alpha^* = 0, \tag{64}$$

$$\partial_\beta P_{\alpha\beta}^* = -\tilde{\gamma}(J_\alpha^* - \rho u_\alpha^E). \tag{65}$$

Using the assumption $P_{\alpha\beta}^* = P_{\alpha\beta}^{eq} = v_T^2 \rho \delta_{\alpha\beta} + \frac{1}{2}(u_\alpha^E J_\beta + u_\beta^E J_\alpha)$, and the definition (58) of J_α^*, we arrive at the equations

$$\partial_\alpha J_\alpha^* = 0, \tag{66}$$

$$v_T^2 \partial_\alpha \rho + \frac{1}{2 - \gamma\Delta t}[-\gamma\Delta t u_\alpha^E u_\beta^E \partial_\beta \rho + u_\beta^E \partial_\beta J_\alpha^*] = -\tilde{\gamma}(J_\alpha^* - \rho u_\alpha^E) \tag{67}$$

for the redefined variables ρ, J_α^*. Note that in this case $\tilde{\gamma}$ must be identified with γ_0 above. Using the equilibrium result $J_\alpha^* = 0$, Eq. (67) easily yields an exponential solution for $\rho(x)$ in dimension 1, from which we can derive the simulated diffusion coefficient D_{sim} as

$$D_{sim} = \frac{v_T^2}{\gamma_0} - \frac{\Delta t}{2\gamma_0^2}(a_0^E)^2. \tag{68}$$

The first term is Einstein's relation and the second gives a correction which is small for vanishing external fields. The result (68) is in accordance with the values reported in Fig. 2 since the correction is larger for small γ_0. Equation (68) can also be written as

$$D_{sim} = D_0\left[1 - \frac{\gamma_0 \Delta t}{2}\left(\frac{u^E}{v_T}\right)^2\right] \tag{69}$$

where $u^E = a_0^E/\gamma_0$. Then another way of interpreting the correction is to say that our numerical scheme is increasingly valid in the low Mach number regime, i.e., u^E must be small compared to v_T, which numerically is $1/\sqrt{3} \simeq 0.6$ for D1Q3 and most common lattices.

Summarizing, we have found that the scheme works, but the theoretical range of parameters must be restricted. The physical friction γ_0 which can be simulated must be such that $0 < \gamma_0 \Delta t < 1$. A small γ_0 is appropriate to obtain a discrete evolution closer to the continuous one, but it must not be too small compared to the external acceleration a_0^E since otherwise the low Mach number assumption would fail. As a final remark, in the case of spatially dependent forces, this must be true for all the points of the system, as we show in the next section.

B. Further examples

In this section we consider two more complicated systems where a BGK collision operator is also present. The systems are described by the combined FP and BGK kinetic equation

$$\frac{df}{dt} = \hat{C}^{FP}[f] + \hat{C}^{BGK}[f] \tag{70}$$

where as in Eq. (1) the total derivative is $d/dt \equiv \partial_t + v_\alpha \partial_\alpha + a_\alpha^E \partial_{v_\alpha}$ and the BGK collision operator is

$$\hat{C}^{BGK}[f] = -\frac{1}{\tau}(f - f^M). \tag{71}$$

The function $f^M = \rho\omega(\mathbf{v} - \mathbf{u})$ is the Maxwell distribution. It contains the density $\rho(\mathbf{x}, t)$ and the velocity $\mathbf{u}(\mathbf{x}, t)$, which

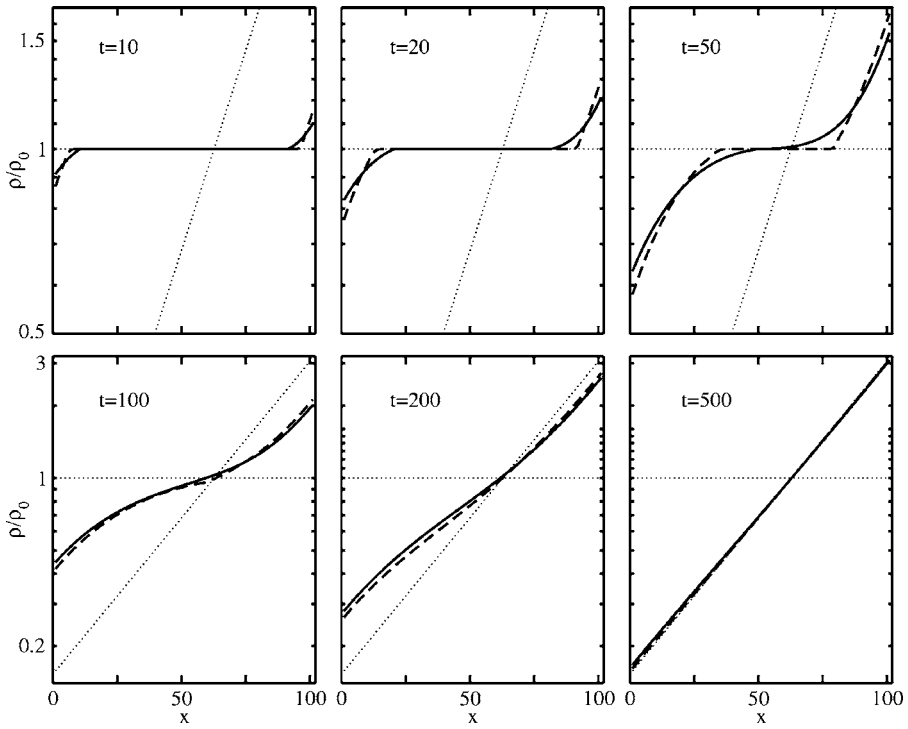

FIG. 3. Log-linear graphs of the normalized density $\rho(x)/\rho_0$ as function of the position x at six different times for a 1D confined system with friction $\gamma_0=0.05/\Delta t$ under the influence of an external acceleration $a_0^E=0.01\Delta x/\Delta t^2$. The system is simulated with a D1Q3 grid of 101 points, and is initially prepared at a homogeneous density ρ_0 (horizontal dotted line in the figures) and no initial velocity. When the external field is applied, the system gradually evolves to the barometric law Eq. (63) and represented as a diagonal dotted line in the figures. We show the evolution for a pure FP collision operator ($\Delta t/\tau=0$, full line) and combined with a BGK operator ($\Delta t/\tau=1.9$, dashed line). Time is in units of Δt and position in units of Δx.

depend self-consistently on f via the definitions (12). The discretization procedure of Sec. II can also be applied to the combined equation (70). The resulting lattice BGK part is well documented in the literature [24,25]. As for the lattice FP equation (18), we also consider a second-order ($K=2$) BGK scheme. Given the previous considerations on the numerical limits of the algorithm, we empirically choose external fields small enough not to break the low Mach number assumption. The BGK operator Eq. (71) with a single relaxation time τ accounts for collisions between particles, and possibly hydrodynamic interactions. The stability analysis of Sec. III can be carried over straightforwardly to this combined case, giving the constraint $0<2\gamma\Delta t+\Delta t/\tau<2$, where $\gamma\Delta t$ in our scheme is given by Eq. (61). Given a value of γ_0 in accordance to the previous subsection, we can then afford a value of $\Delta t/\tau$ up to $2-2\gamma_0\Delta t$ and slightly above.

As a first example, consider the one-dimensional (1D) system of the previous subsection with reflecting boundaries and simulations on the D1Q3 lattice with 101 lattice sites. We focus here on the time-dependent approach to equilibrium. Such a condition corresponds to sedimentation caused by gravity. We report the results in Fig. 3. Interestingly we find that the presence of BGK collisions delays the start of the relaxation, but then makes it converge faster once started. The horizontal plateau of the density profiles at the early stages is due to the finite propagation velocity of lattice schemes, which are restricted in this case to only three possibilities. If one is interested in studying these effects a different lattice with a larger number of discrete velocities must be employed.

In the second case, we consider the 2D system represented in Fig. 4, where we combine sedimentation and a centrifugal force. We apply bounce-back reflecting boundaries on a D2Q9 lattice [6] of 21×41 points. We consider a system with friction $\gamma_0=0.1/\Delta t$ under the influence of a gravity $g=0.01\Delta x/\Delta t^2$ and a centrifugal force due to a rotation of frequency $\omega_r=0.03/\Delta t$. Here Δt is the time unit and Δx the lattice spacing. Also at the borders the low Mach number assumption is satisfied. We report the results in Fig. 5. At short times the pure FP system departs earlier from the homogeneous situation. However, at longer times the presence of BGK collisions accelerates the approach to equilibrium. Around $t=400$ both systems are converged and the final profiles are in agreement with the analytical Boltzmann law

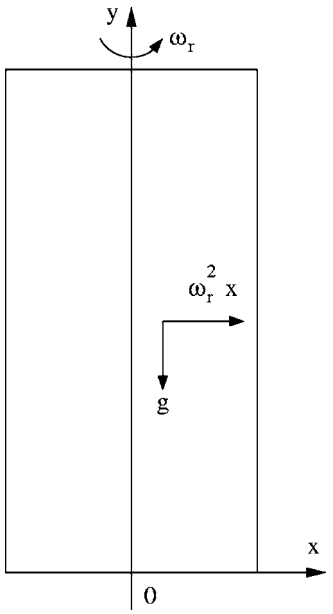

FIG. 4. The 2D confined system. Sedimentation under gravity is combined with a centrifugal force. The external acceleration is a combination of the constant g and the linear escape term $\omega_r^2 x$.

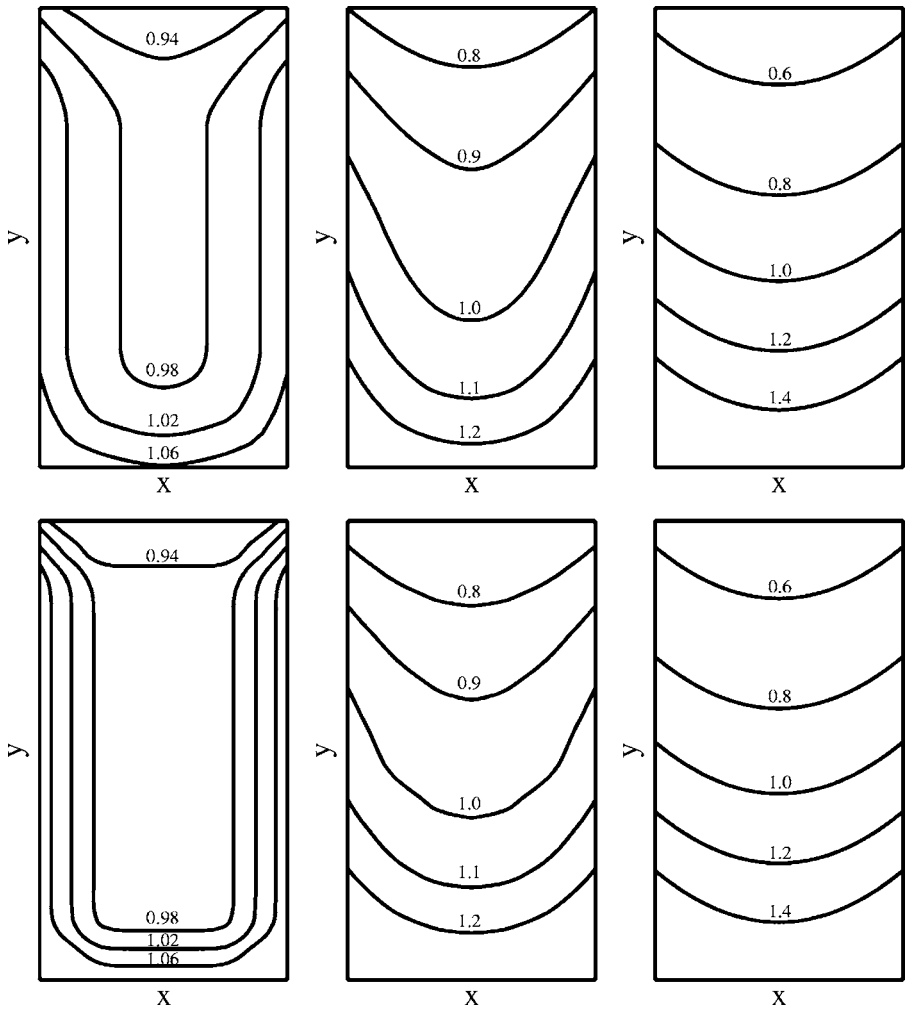

FIG. 5. Contour plots of the normalized density $\rho(x,y)/\rho_0$ at three different times for a simulation on a D2Q9 lattice of 21×41 sites with reflecting boundary conditions. The system is initially homogeneous at density ρ_0 and the velocity field is set to zero. We show the evolution for a pure FP collision operator ($\Delta t/\tau=0$, top figures) and combined with a BGK operator ($\Delta t/\tau=1.8$, bottom figures). Left panels show the evolution at the early stage ($t=10$), the middle ones at intermediate stage ($t=40$), and the right panels at steady state ($t=400$), where both systems have converged to the analytical Boltzmann law Eq. (72). Time is in units of Δt and positions in units of the lattice spacing Δx. The contour lines are a spline interpolation.

$$\rho_{eq}(x,y) \propto \exp\left[-\left(gy-\frac{\omega_r^2}{2}x^2\right)/v_T^2\right] \tag{72}$$

which combines the parabolic behavior due to centrifugation with the exponential one in the perpendicular direction due to gravity. The proportionality constant in Eq. (72) can be derived from the conservation of the total number of particles, i.e., $\int dx\,dy\,\rho(x,y,t=0)=\int dx\,dy\,\rho_{eq}(x,y)$. The explicit time dependence at fixed points in space as well as a direct comparison of the steady state with Eq. (72) is reported in Fig. 6 for the pure FP system. The findings are in accordance with the ones of the previous example. Also here, the flatness of the density profile at early times is caused by the finite number of velocities in the lattice scheme.

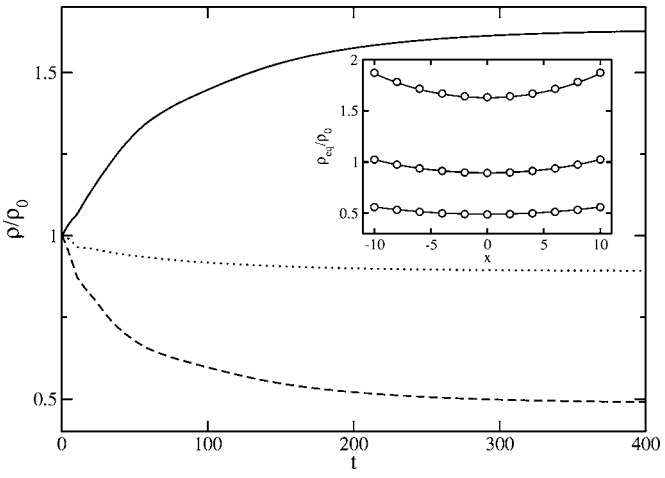

FIG. 6. Time evolution of the normalized density $\rho(x,y)/\rho_0$ for the same system as in Fig. 5 in the case of a pure FP collision operator. The height of the box is $L_y=40$ lattice units and three different points are shown: $x=0$, $y=0$ (solid line), $x=0$, $y=L_y/2$ (dotted line), $x=0$, $y=L_y$ (dashed line). In the inset the steady state at $t=400$ (open circles) is compared with the analytical Boltzmann law Eq. (72) and solid lines in the plot. The top points are at $y=0$, the middle ones at $y=L_y/2$, and the bottom ones at $y=L_y$. Time is in units of Δt and positions in units of the lattice spacing Δx.

VII. CONCLUSION

In order to describe the time evolution of highly asymmetric systems, involving widely different length and time scales, like colloidal dispersions, we have extended the lattice-Boltzmann formalism for the description of fluid flow by replacing the standard BGK collision operator by a discretized Fokker-Planck operator to account for the dissipative coupling of large solutes to a continuum solvent, without resolving the molecular scale of the latter. Using an expan-

sion of the continuous one-particle distribution function in a truncated Gauss-Hermite basis, as well as standard quadratures with appropriately chosen weights, we were able to reduce the initial continuous Fokker-Planck equation to a simple matrix form. The stability of the discrete time evolution is determined by the diagonal elements of the triangular collision matrix, which are proportional to the friction coefficient γ. A standard Chapman-Enskog expansion leads back to the usual conservation equations derived from the continuous FP equation in the limit $\Delta t \to 0$. For finite time steps Δt, the correct continuum equations are recovered by properly redefining the hydrodynamic variables, i.e., by introducing the starred current and stress tensor of Eqs. (58). This leads then to the lattice Fokker-Planck algorithm of Sec. V.

This algorithm was first tested against known analytical results for the time evolution of simple model systems. The numerical efficiency was tested in the nontrivial case of colloid sedimentation in the presence of gravity and a centrifugal force. We intend to use the LFP algorithm to investigate ion translocation through heterogeneous nanopores, ion transport in swollen clays, and various applications in dissipative colloid dynamics. These applications will benefit from the extensive experience gained over the years with the related LB method.

Due to the well-known mapping between the Fokker-Planck and the imaginary time Schrödinger equation [17], the present LFP scheme is also applicable to the solution of ground-state quantum problems.

The present LFP scheme has a number of limitations. First of all, the Fokker-Planck equation itself is never fully rigorous, since a separation of time scales is never complete, as had already been recognized by Lorentz [41] so that non-Markovian corrections are always present [42]. Second, to account for collisions between particles, a BGK term may be added to the discrete FP operator, as stressed several times in this paper, and illustrated in two of the numerical examples (see Figs. 3 and 5). However, it is not clear how such a term could account for the long-range hydrodynamic interactions between Brownian particles induced by the solvent backflow. A third limitation emerges from the stability analysis, which restricts the range of possible values of the inverse time scales γ (associated with the FP operator) and $1/\tau$ (characterizing the BGK operator). Clearly there is a need for an algorithm valid to higher order in Δt. Work along these lines is in progress.

The lattice Fokker-Planck equation belongs to the family of mesoscopic particle schemes for complex flows. It is hence appropriate to outline the differences with some of the already existing methods.

Multicomponent lattice-Boltzmann for mixtures [21–23] is the closest to the LFP method. For an application see also [11]. Two coupled kinetic equations for solute and solvent can be solved by lattice BGK algorithms which take as input the relaxation times τ_{solute} and $\tau_{solvent}$. A combined LFP-BGK method uses instead τ_{solute} and the friction coefficient γ, employing a one-component description and treating the solvent implicitly. This approach becomes more efficient when the relaxation times of solute and solvent are highly asymmetric (separation of time scales) as in the case of colloidal suspensions. Naturally, multicomponent schemes can also be extended to the LFP method, where more than one solute is present in the solvent.

The method of Capuani *et al.* [12] is a model to simulate general nonideal fluid mixtures at the hydrodynamic level. Convection-diffusion equations for the densities and currents of each species are coupled to the Navier-Stokes equation for the whole fluid. When one of the species is a solvent an approximation can be made, and the solvent diffusion equation is neglected. So for a system of ν species plus solvent, $\nu+1$ equations must be solved. The lattice-Boltzmann method enters here as an efficient way to solve the hydrodynamic equation. In contrast, a generalized multicomponent LFP method for ν species would require ν equations, because the solvent would enter in each of them as a Fokker-Planck collision term. Being at the kinetic level, the LFP description can in principle compute the moments of the distribution function to any desired order, and this is not limited to the lowest-order hydrodynamic moments, i.e., density and current. The FP term is also supposed to take into account inelastic collisions of solute particles with confining surfaces. In [12] the nonideal part of the model is included self-consistently via an additional closure equation, e.g., the Poisson equation in the case of polyelectrolytes. This can also be included in our model through a self-consistent external field. Such an implementation is currently under investigation.

Particulate methods for solutions differ more substantially from the LFP approach. In dissipative particle dynamics [43] coarse-grained solute particles undergo a combination of conservative, dissipative and random forces. As in the LFP method the solvent is treated implicitly, but at variance with the LFP approach the time evolution of distribution functions and the hydrodynamic fields must be computed from averages over many realizations. At the kinetic level of the LFP method, stochastic components are not present and direct access to the moments of the distribution function is available. The same problem is present in stochastic rotation dynamics [44,45] which also adds solvent particles, even though the solvent-solvent interaction is treated in a faster stochastic way. Particulate methods where the solvent is treated as a hydrodynamic continuum also exist. The hydrodynamics is then treated by Stokesian dynamics or the lattice-Boltzmann method [15]. However, proper handling of this kind of solvent is not trivial because of the particles being represented as moving boundaries and the presence of lubrication forces. The LB solvent can also be formulated to include thermal fluctuations [46]. It will be interesting to explore whether the lattice Fokker-Planck equation represents an alternative, possibly more efficient, way of incorporating statistical fluctuations within the framework of an on-grid and deterministic lattice kinetic scheme.

The more detailed a description one chooses, the more expensive the simulations become. In systems with a separation of time scales it is known that a coarse-grained model for the faster and less relevant species (the solvent) must be adopted, and one must simulate at the time scale of the mesoscopic species (the solute). We propose here to treat the solvent implicitly as a source of friction and thermal noise for a solute described at the kinetic level of the distribution function. The LFP method is the simplest of the above men-

tioned methods, but easier to implement, and faster. We plan to report on such issues in future publications.

ACKNOWLEDGMENTS

D.M. acknowledges financial support from the University of Rome La Sapienza and from Schlumberger Cambridge Research. B.R. acknowledges financial support from the Ecole Normale Supérieure and the Agence Nationale pour la Gestion des Déchets Radioactifs (ANDRA, France).

APPENDIX A: *D*-DIMENSIONAL HERMITE POLYNOMIALS

A complete set of orthonormal polynomials in D variables can be obtained by products of Hermite polynomials in a single variable. A detailed presentation can be found in the work of Grad [47]. Here we sketch the basic notions and concentrate on the relations which are useful in the present work.

Consider the space of real functions $f(\mathbf{x})$ of D variables for which the integral $\int d\mathbf{v}\, \omega(\mathbf{v}) f(\mathbf{v})^2$ exists, where $\omega(\mathbf{v})$ is the Gaussian weight function defined by Eq. (5). A D-dimensional Hermite polynomial of order l is a tensor $\mathcal{H}^{(l)}_{\underline{\alpha}}(\mathbf{x})$ of rank l. Each component is a polynomial function in this space. These polynomials form an orthogonal set in the sense

$$\int d\mathbf{v}\, \omega(\mathbf{v}) \frac{1}{v_T^{l+m}} \mathcal{H}^{(l)}_{\underline{\alpha}}(\mathbf{v}) \mathcal{H}^{(m)}_{\underline{\beta}}(\mathbf{v}) = \delta_{lm} \delta^{(l)}_{\underline{\alpha}\underline{\beta}} \tag{A1}$$

where the quantity $\delta^{(l)}_{\underline{\alpha}\underline{\beta}}$ is zero unless the subscripts $\underline{\alpha} = \alpha_1, \ldots, \alpha_l$ are a permutation of $\underline{\beta} = \beta_1, \ldots, \beta_l$. It is a sum of $l!$ terms, each one being a product of l Kronecker δ's with the subscripts given by all the possible permutations of indices from the two sets $\underline{\alpha}$ and $\underline{\beta}$. The first few polynomials read [1]

$$\mathcal{H}^{(0)}(\mathbf{v}) = 1, \tag{A2}$$

$$\mathcal{H}^{(1)}_{\alpha}(\mathbf{v}) = v_\alpha, \tag{A3}$$

$$\mathcal{H}^{(2)}_{\alpha\beta}(\mathbf{v}) = v_\alpha v_\beta - v_T^2 \delta_{\alpha\beta}, \tag{A4}$$

$$\mathcal{H}^{(3)}_{\alpha\beta\gamma}(\mathbf{v}) = v_\alpha v_\beta v_\gamma - v_T^2 (v_\alpha \delta_{\beta\gamma} + v_\beta \delta_{\alpha\gamma} + v_\gamma \delta_{\alpha\beta}), \tag{A5}$$

$$\begin{aligned} \mathcal{H}^{(4)}_{\alpha\beta\gamma\delta}(\mathbf{v}) = {} & v_\alpha v_\beta v_\gamma v_\delta - v_T^2 (v_\alpha v_\beta \delta_{\gamma\delta} + v_\alpha v_\gamma \delta_{\beta\delta} + v_\alpha v_\delta \delta_{\beta\gamma} \\ & + v_\beta v_\gamma \delta_{\alpha\delta} + v_\beta v_\delta \delta_{\alpha\gamma} + v_\gamma v_\delta \delta_{\alpha\beta}) + v_T^4 (\delta_{\alpha\beta}\delta_{\gamma\delta} \\ & + \delta_{\alpha\gamma}\delta_{\beta\delta} + \delta_{\alpha\delta}\delta_{\beta\gamma}). \end{aligned} \tag{A6}$$

Hermite polynomials form a complete set and the expansion (4) is valid, where the coefficients are given by Eq. (6). In $D=1$ the polynomials defined here reduce to the so-called Hermite-Chebyshev polynomials, which differ in normalization from the usual Hermite polynomials [48]. The derivative of Hermite polynomials satisfies two important properties. The first relates an Hermite polynomial of degree l to one of degree $l-1$,

$$\partial_{v_\beta} \mathcal{H}^{(l)}_{\underline{\alpha}}(\mathbf{v}) = \delta_{\beta\alpha_1} \mathcal{H}^{(l-1)}_{\alpha_2,\ldots,\alpha_l}(\mathbf{v}) + \cdots + \delta_{\beta\alpha_l} \mathcal{H}^{(l-1)}_{\alpha_1,\ldots,\alpha_{l-1}}(\mathbf{v}). \tag{A7}$$

The second is the recurrence relation

$$\partial_{v_\beta} \mathcal{H}^{(l)}_{\underline{\alpha}}(\mathbf{v}) = \frac{1}{v_T^2} [v_\beta \mathcal{H}^{(l)}_{\underline{\alpha}}(\mathbf{v}) - \mathcal{H}^{(l+1)}_{\beta\underline{\alpha}}(\mathbf{v})] \tag{A8}$$

where $\beta\underline{\alpha}$ denotes the $l+1$ indices $\beta\alpha_1, \ldots, \alpha_l$.

Making use of the quadratures Eqs. (10) in Sec. II, integrals of products of Hermite polynomials and a Gaussian can be rewritten as discrete sums on lattice vectors. The maximum order of the polynomial involved is dictated by the order of the quadratures. In the practical case of interest here, a quadrature of order 4 is used in the model of Eq. (18), where $K=2$. The orthonormality relations Eq. (A1) become then the discrete sum rules

$$\sum_i w_i = 1, \tag{A9}$$

$$\sum_i w_i v_{i\alpha} v_{i\beta} = v_T^2 \delta_{\alpha\beta}, \tag{A10}$$

$$\sum_i w_i (v_{i\alpha} v_{i\beta} - v_T^2 \delta_{\alpha\beta})(v_{i\gamma} v_{i\delta} - v_T^2 \delta_{\gamma\delta}) = v_T^4 (\delta_{\alpha\gamma}\delta_{\beta\delta} + \delta_{\alpha\delta}\delta_{\beta\gamma}), \tag{A11}$$

and the remaining combinations, such as $\Sigma_i w_i v_{i\alpha}$, etc., are simply 0. From the last Eq. (A11) we can derive the fourth-order tensor formula

$$\sum_i w_i v_{i\alpha} v_{i\beta} v_{i\gamma} v_{i\delta} = v_T^4 (\delta_{\alpha\beta}\delta_{\gamma\delta} + \delta_{\alpha\gamma}\delta_{\beta\delta} + \delta_{\alpha\delta}\delta_{\beta\gamma}). \tag{A12}$$

APPENDIX B: EIGENFUNCTIONS OF THE *D*-DIMENSIONAL FOKKER-PLANCK OPERATOR

The D-dimensional Hermite polynomials defined in the previous section can be used to construct eigenfunctions of the Fokker-Planck operator $\hat{C}^{FP}[f]$ of Eq. (1) in the form of products $\omega(\mathbf{v})\mathcal{H}^{(l)}_{\underline{\alpha}}(\mathbf{v})$.

Using the fact that for a Gaussian

$$\partial_{v_\alpha} \omega(\mathbf{v}) = -\frac{v_\alpha}{v_T^2} \omega(\mathbf{v}) \tag{B1}$$

we can write for the action of $\hat{C}^{FP}$ on these functions

[1] The Hermite polynomials $\mathcal{H}^{(l)}_{\underline{\alpha}}(\mathbf{v})$ defined here can be considered as a dimensional-explicit version of the polynomials $\bar{\mathcal{H}}^{(l)}_{\underline{\alpha}}(\mathbf{v})$ defined by Grad [47]. The relation $\mathcal{H}^{(l)}_{\underline{\alpha}}(\mathbf{v}) = v_T^l \bar{\mathcal{H}}^{(l)}_{\underline{\alpha}}(\mathbf{v}/v_T)$ exists between the two, where v_T has the dimension of the velocity $\mathbf{v}$.

$$\hat{C}^{FP}[\omega(\mathbf{v})\mathcal{H}^{(l)}_{\underline{\alpha}}(\mathbf{v})] = \gamma\partial_{v_\beta}(v_\beta + v_T^2\partial_{v_\beta})[\omega(\mathbf{v})\mathcal{H}^{(l)}_{\underline{\alpha}}(\mathbf{v})] = \gamma\omega(\mathbf{v}) \times(-v_\beta\partial_{v_\beta} + v_T^2\partial_{v_\beta}\partial_{v_\beta})\mathcal{H}^{(l)}_{\underline{\alpha}}(\mathbf{v}). \quad \text{(B2)}$$

Because of relation (A8), we can write

$$v_T^2\partial_{v_\beta}\partial_{v_\beta}\mathcal{H}^{(l)}_{\underline{\alpha}}(\mathbf{v}) = D\mathcal{H}^{(l)}_{\underline{\alpha}}(\mathbf{v}) + v_\beta\partial_{v_\beta}\mathcal{H}^{(l)}_{\underline{\alpha}}(\mathbf{v}) - \partial_{v_\beta}\mathcal{H}^{(l+1)}_{\underline{\beta\alpha}}(\mathbf{v}). \quad \text{(B3)}$$

Using then property (A7) it is easy to prove that

$$\partial_{v_\beta}\mathcal{H}^{(l+1)}_{\underline{\beta\alpha}}(\mathbf{v}) = -(l+D)\mathcal{H}^{(l)}_{\underline{\alpha}}(\mathbf{v}). \quad \text{(B4)}$$

Bringing all the above relations together we get

$$\hat{C}^{FP}[\omega(\mathbf{v})\mathcal{H}^{(l)}_{\underline{\alpha}}(\mathbf{v})] = -\gamma l\omega(\mathbf{v})\mathcal{H}^{(l)}_{\underline{\alpha}}(\mathbf{v}) \quad \text{(B5)}$$

which is the eigenvalue property we wanted to prove. From this it is immediate to prove relation (16a) using (25) and the orthonormality of the polynomials.

We can use the above results to prove also relation (16b). From Eqs. (B1) and (A8) we get

$$\hat{C}^{ext}[\omega(\mathbf{v})\mathcal{H}^{(l)}_{\underline{\alpha}}(\mathbf{v})] = -a^E_\beta\partial_{v_\beta}[\omega(\mathbf{v})\mathcal{H}^{(l)}_{\underline{\alpha}}(\mathbf{v})] = \frac{\omega(\mathbf{v})}{v_T^2}a^E_\beta\mathcal{H}^{(l+1)}_{\underline{\beta\alpha}}(\mathbf{v}), \quad \text{(B6)}$$

from which, using the expansion (4),

$$\begin{aligned}
&\int d\mathbf{v}\,\mathcal{H}^{(m)}_{\underline{\gamma}}(\mathbf{v})\hat{C}^{ext}[f] \\
&= \sum_{l=0}^{\infty}\frac{F^{(l)}_{\underline{\alpha}}}{v_T^{2l}l!}\int d\mathbf{v}\,\mathcal{H}^{(m)}_{\underline{\gamma}}(\mathbf{v})\hat{C}^{ext}[\omega(\mathbf{v})\mathcal{H}^{(l)}_{\underline{\alpha}}(\mathbf{v})] \\
&= \sum_{l=0}^{\infty}\frac{F^{(l)}_{\underline{\alpha}}}{v_T^{2l}l!}\frac{a^E_\beta}{v_T^2}\int d\mathbf{v}\,\mathcal{H}^{(m)}_{\underline{\gamma}}(\mathbf{v})\omega(\mathbf{v})\mathcal{H}^{(l+1)}_{\underline{\beta\alpha}}(\mathbf{v}) \\
&= \frac{1}{(m-1)!}F^{(m-1)}_{\underline{\alpha}}a^E_\beta\delta^{(m)}_{\underline{\gamma},\underline{\beta\alpha}} \\
&= a^E_{\gamma_1}F^{(m-1)}_{\gamma_2,\ldots,\gamma_m} + \cdots + a^E_{\gamma_m}F^{(m-1)}_{\gamma_1,\ldots,\gamma_{m-1}}
\end{aligned} \quad \text{(B7)}$$

where we used Eq. (A1) and the fact that $F^{(m-1)}$ is invariant under permutations of its $m-1$ indices.

[1] P. Résibois and M. De Leener, *Classical Kinetic Theory of Fluids* (Wiley, New York, 1977).
[2] J. P. Hansen and I. R. McDonald, *Theory of Simple Liquids*, 2nd ed. (Academic Press, London, 1986).
[3] D. Montgomery and D. Tidman, *Plasma Kinetic Theory* (McGraw-Hill, New York, 1964).
[4] C. Cercignani, *The Boltzmann Equation and Its Applications* (Springer-Verlag, New York, 1988).
[5] P. Bhatnagar, E. Gross, and M. Krook, Phys. Rev. **94**, 511 (1954).
[6] S. Succi, *The Lattice Boltzmann Equation for Fluid Dynamics and Beyond* (Oxford University Press, Oxford, 2001).
[7] R. Benzi, S. Succi, and M. Vergassola, Phys. Rep. **222**, 145 (1992).
[8] D. A. Wolf-Gladrow, *Lattice-Gas Cellular Automata and Lattice Boltzmann Models: An Introduction* (Springer, Berlin, 2000).
[9] H. Chen, S. Kandasamy, S. Orszag, R. Shock, S. Succi, and V. Yakhot, Science **301**, 633 (2003).
[10] J. Harting, J. Chin, M. Venturoli, and P. V. Coveney, Philos. Trans. R. Soc. London, Ser. A **363**, 1895 (2005).
[11] N. González-Segredo and P. V. Coveney, Phys. Rev. E **69**, 061501 (2004).
[12] F. Capuani, I. Pagonabarraga, and D. Frenkel, J. Chem. Phys. **121**, 973 (2004).
[13] S. Melchionna and S. Succi, Comput. Phys. Commun. **169**, 203 (2005).
[14] A. Dupuis, D. Marenduzzo, E. Orlandini, and J. M. Yeomans, Phys. Rev. Lett. **95**, 097801 (2005).
[15] A. Ladd and R. Verberg, J. Stat. Phys. **104**, 1191 (2001).
[16] K. Stratford, R. Adhikari, I. Pagonabarraga, J.-C. Desplat, and M. E. Cates, Science **309**, 2198 (2005).
[17] H. Risken, *The Fokker-Planck Equation* (Springer-Verlag, Berlin, 1989).
[18] S. Succi, S. Melchionna, and J.-P. Hansen, Int. J. Mod. Phys. C **17**, 459 (2006).
[19] S. Melchionna, S. Succi, and J.-P. Hansen, Phys. Rev. E **73**, 017701 (2006).
[20] P. Turq, F. Lantelme, and H. L. Friedman, J. Chem. Phys. **66**, 3039 (1977).
[21] V. Sofonea and R. F. Sekerka, Physica A **299**, 494 (2001).
[22] L.-S. Luo and S. S. Girimaji, Phys. Rev. E **66**, 035301(R) (2002).
[23] L.-S. Luo and S. S. Girimaji, Phys. Rev. E **67**, 036302 (2003).
[24] X. Shan and X. He, Phys. Rev. Lett. **80**, 65 (1998).
[25] N. S. Martys, X. Shan, and H. Chen, Phys. Rev. E **58**, 6855 (1998).
[26] X. He and L.-S. Luo, Phys. Rev. E **55**, R6333 (1997).
[27] H. Grad, Commun. Pure Appl. Math. **2**, 331 (1949).
[28] S. Ansumali and I. V. Karlin, Phys. Rev. E **66**, 026311 (2002).
[29] S. Ansumali, I. V. Karlin, and H. C. Öttinger, Europhys. Lett. **63**, 798 (2003).
[30] J. L. Skinner and P. G. Wolynes, J. Chem. Phys. **72**, 4913 (1980).
[31] A. H. Stroud, *Approximate Calculation of Multiple Integrals* (Prentice-Hall, Englewood Cliffs, NJ, 1971).
[32] A. N. Gorban and I. V. Karlin, Phys. Rev. E **54**, R3109 (1996).
[33] F. Higuera and J. Jiménez, Europhys. Lett. **9**, 663 (1989).
[34] F. Higuera, S. Succi, and R. Benzi, Europhys. Lett. **9**, 345 (1989).
[35] R. A. Worthing, J. Mozer, and G. Seeley, Phys. Rev. E **56**, 2243 (1997).
[36] J.-P. Rivet and J. P. Boon, *Lattice Gas Hydrodynamics* (Cambridge University Press, Cambridge, U.K., 2005).
[37] C. M. Bender and S. A. Orszag, *Advanced Mathematical Methods for Scientists and Engineers* (Springer-Verlag, New York,

1999).
[38] Z. Guo, C. Zheng, and B. Shi, Phys. Rev. E **65**, 046308 (2002).
[39] S. Donath (unpublished).
[40] K. Iglberger, BS thesis, Institut für Informatik, University of Erlangen-Nuremberg, Germany, 2003, (unpublished).
[41] For a discussion, see, e.g., L. Bocquet and J. P. Hansen, in *Dynamics: Models and Kinetic Methods for Non-Equilibrium Many Body Systems*, edited by J. Karkheck, NATO Advanced Studies Institute, Series E: Applied Science (Kluwer, Dordrecht, The Netherlands, 2000), Vol. 371.
[42] L. Bocquet and J. Piasecki, J. Stat. Phys. **87**, 1005 (1997).
[43] For a recent application to polyelectrolyte-surfactant systems, see R. D. Groot, J. Chem. Phys. **118**, 11265 (2003).
[44] A. Malevanets and R. Kapral, J. Chem. Phys. **112**, 7260 (2000).
[45] For a recent application, see J. T. Padding and A. A. Louis, Phys. Rev. Lett. **93**, 220601 (2004).
[46] A. J. C. Ladd, Phys. Rev. Lett. **70**, 1339 (1993).
[47] H. Grad, Commun. Pure Appl. Math. **2**, 325 (1949).
[48] *Handbook of Mathematical Functions with Formulas, Graphs, and Mathematical Tables*, edited by M. Abramowitz and I. A. Stegun (Dover, New York, 1972).